Histone deacetylase inhibition sensitizes p53-deficient B-cell precursor acute lymphoblastic leukemia to chemotherapy

Willem P.J. Cox,[1] Nils Evander,[1] Dorette S. van Ingen Schenau,[1] Gawin R. Stoll,[1] Nadia Anderson,[1] Lieke de Groot,[1] Kari J.T. Grünewald,[1] Rico Hagelaar,[1,2] Miriam Butler,[1] Roland P. Kuiper,[1,3] Laurens T. van der Meer[1#] and Frank N. van Leeuwen[1#]

[1]Princess Máxima Center for Pediatric Oncology and [2]Oncode Institute and [3]Department of Genetics, Utrecht University Medical Center, Utrecht University, Utrecht, the Netherlands

[#]LTvdM and FNvL contributed equally as senior authors.

Correspondence: F.N. van Leeuwen
f.n.vanleeuwen@prinsesmaximacentrum.nl

Received: August 17, 2023.
Accepted: December 13, 2023.
Early view: December 21, 2023.

https://doi.org/10.3324/haematol.2023.284101

SUPPLEMENTAL METHODS

Cell models

The parental BCP-ALL cell lines Nalm6 (ACC 548) and RCH-ACV (ACC 128) were obtained from DSMZ. Using CRISPR/Cas9, isogenic $p53^{KO}$ and $p53^{WT}$ single-cell clones were generated, validated (Table S2), and combined into pools to rule out clonal differences. Cell line identity was validated by DNA fingerprinting. Cells are cultured for a maximum of three months and tested every six weeks for the presence of *mycoplasma*. For combination assay and *in vivo* purposes, cells were transduced with either GFP- or mCherry-luciferase constructs and FACS sorted to obtain pure populations. Patient-derived xenograft (PDX) were generated as previously described[1], and their TP53 status was previously determined by in-house single-molecule molecular inversion probes (smMIP) assay, and SALSA digitalMLPA Acute Lymphoblastic Leukemia Probemix (D007; performed by MRC Holland).

Reagents

Prednisolone (*di-Adreson-F*) was acquired from ACE Pharmaceuticals; cytarabine (*Cytarabine Accord*) from Accord Healthcare; doxorubicin (APOSBID0120) from Apollo Scientific; tucidinostat (13686) and cyclophosphamide (H714675) from Cayman Chemicals; dexamethasone (*Dexamethason CF*) from Centrafarm; Romidepsin (DCAPI1434) and nutlin-3 (DC3125) from DC Chemicals; 6-mercaptopurine (HY-13677), bortezomib (HY-10227), calicheamicin (HY-19609), L-asparaginase (*Spectrilla*) from medac; entinostat (HY-12163) and vincristine (HY-N0488) from MedChemExpress; inotuzumab ozogamicin (*Besponsa*) from Pfizer; actinomycin D (*Cosmegen Lyovac*) from Recordati Rare Diseases; daunorubicin (*Cerubidine*) from Sanofi Genzyme; 6-thioguanine (sc-205587) from Santa Cruz Biotechnology; carfilzomib (S2853) idarubicin (S1228) and mitoxantrone (S1889) from Selleckchem; fludarabine (F9813) from Sigma-Aldrich; etoposide (*Toposin*) and methotrexate (*Emthexate PF*) from Teva Pharmaceuticals.

Drug screening (extended)

Before the screening, the 384-well working plates containing the dissolved drugs were shaken (30 min, RT) and centrifuged (1 min, 350 x *g*). Cells were treated with a dilution series of the drugs on the library plate at final concentrations of 0.1 nM, 1 nM, 10 nM, 100 nM, 1 μM and 10 μM (0.25% DMSO or MQ), with several drugs tested at additional lower concentrations (up to 10 pM) or higher concentrations (up to 200 μM). Negative control samples were treated with DMSO and positive control samples with staurosporine (final concentration of 10 μM). 3-(4,5-dimethylthiazol-2-yl)-2,5-diphenyltetrazolium bromide (MTT) conversion was used as cell readout according to the manufacturer's protocol at T0 (control plate, before the addition of drugs to assay plates) and at T72 (assay plates, 72h after addition of drugs–

readout). Dose-response was estimated per drug and concentration compared with the DMSO-treated cells (set to 100%) and empty controls (set to 0%). The quality of the screenings was approved after assessment of the cell growth (absorbance signal of T72 over T0), the negative, positive, and empty controls.

Quantitative reverse transcription PCR (RT-qPCR)

Total RNA was extracted from cell lines using a NucleoSpin RNA isolation kit (740955, Machery-Nagel). RNA (0.25 μg) was reverse transcribed into cDNA using an iScript cDNA synthesis kit (1708891, Bio-Rad). Each RT-qPCR was performed in two technical duplicates for biological triplicates in a 384-well plate on a CFX96 or CFX384 Touch Real-Time PCR detection system (Bio-Rad) using SsoAdvanced Universal SYBR Green Supermix (1725274, Bio-Rad) according to the manufacturer's instructions. The cycling conditions were 95°C for 3 min, 95°C for 10s, and 60°C for 30s for 40 cycles, followed by melt analysis from 65 to 95°C. Expression levels were normalized to the housekeeping gene TATA-box binding protein (*TBP*).

In vivo study (extended)

At the start of the study, mice were 6-20 weeks-old (median age 6.4 weeks). Mice were housed in individually ventilated cages in groups of 4-6 mice per cage in a room with a 12:12-h light:dark cycle and with free access to food and water (ad libitum). Before engraftment, mice were acclimatized for one week. Randomization was performed via a random number generator. Per group, seven mice were included based on power calculations *a priori* (effect size and standard deviation of photon flux of 0.3 and 0.15, respectively, based on previous experiments). Mice were humanely euthanized by CO2 asphyxiation when the total photon flux exceeded levels of $5x10^{10}$ photons/second.

Data analysis and visualization (extended)

Statistical tests used in each analysis are described in the relevant portions of the Results and Methods sections or figure legends. For several dose-response curves, the shape of the curve did not allow curve fitting and IC50 calculations. Therefore, we calculated the area under the curve (AUC) and tested differences for significance using an unpaired two-tailed t-test or one-way ANOVA with Tukey's multiple comparisons test for viability curves. To test for statistical significance of qRT-PCR results, two-way ANOVA followed by Tukey's multiple comparisons tests were performed per model. p-values smaller than 0.05 were considered statistically significant (*$p<0.05$, **$p<0.01$, ***$p<0.001$, ****$p<0.0001$). Statistical analyses and data visualization were performed using PRISM9 (GraphPad Software Inc., La Jolla CA, United States), FlowJo v10.9 (FlowJo LLC., Ashland OR, United States) or RStudiov4.0.2 (Posit PBC., Boston MA, United States). Synergy scores were calculated using the SynergyFinder Plus R pack-

age based on the ZIP model.[2] Drug screen data analysis was performed with, calculating Area Under the Curve (AUC) values using the *drc extension package* for every drug.[3] Gene set enrichment was performed using GSEAv4.3.2 software.[4, 5] Differential gene expressions were computed using the DESeq2 R package, filtered on p-value and fold changes (excluded $p > 0.05$, and $-0.5 < \log_2 FC < 0.5$), and analyzed using the Venn generator from UGent and Search Tool for the Retrieval of Interacting Genes/Proteins (STRING) v11.5.[6-8] Heatmaps were generated using unsupervised clustering with the ComplexHeatmap R package.[9]

SUPPLEMENTAL FIGURES

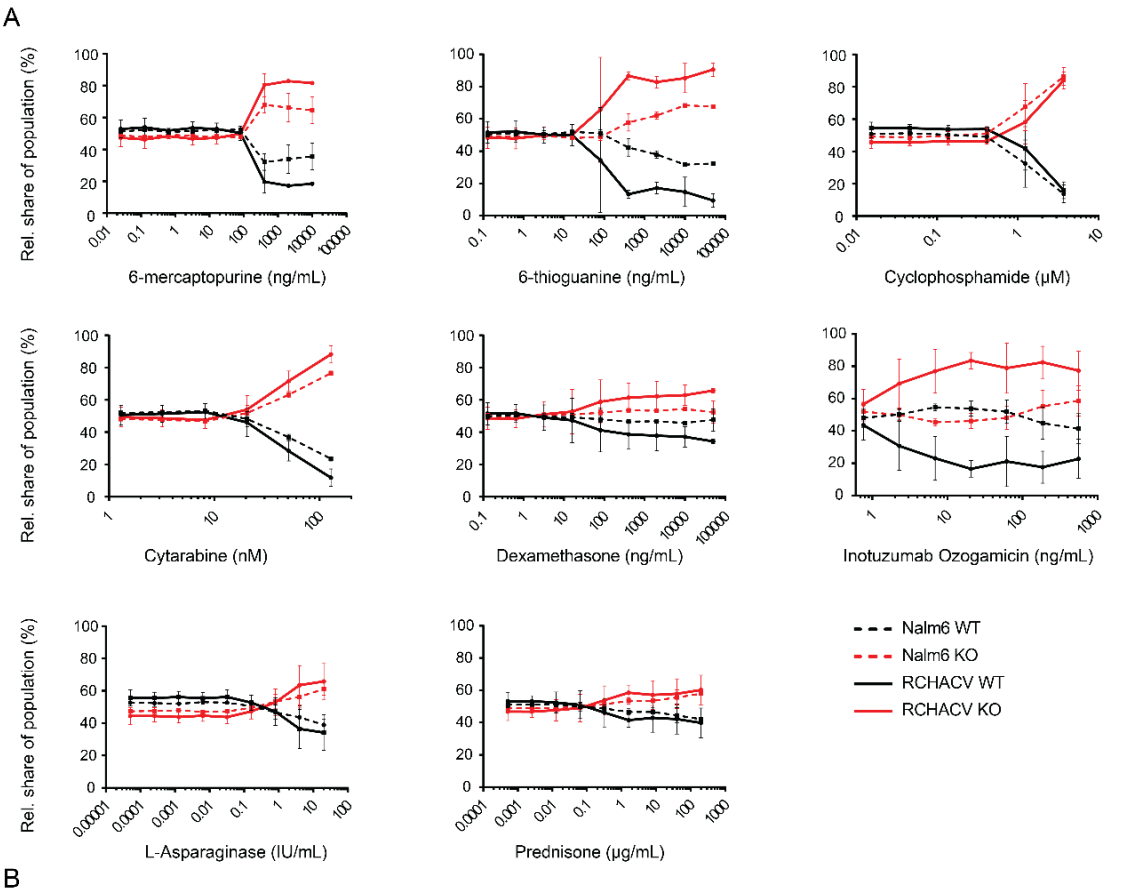

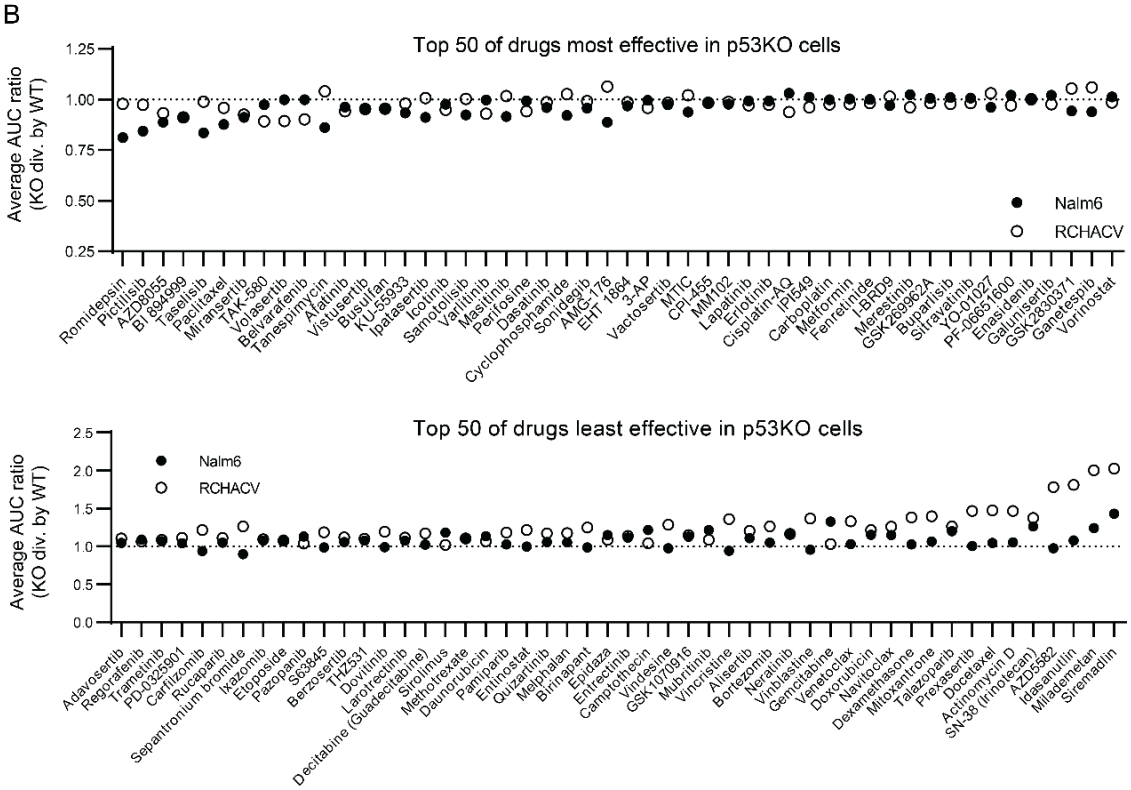

Figure S1 – Loss of p53 confers differential sensitivity to commonly used cancer therapeutics. (A) Combination assay results showed the relative percentage of fluorescent Nalm6 and RCHACV $p53^{KO}$ cells (expressing mCherry) when combined with their $p53^{WT}$ counterparts (expressing GFP) in one culture and exposed to the indicated drugs for 72 hours. GFP and mCherry fluorescence was measured by flow cytometry. Each data point represents a mean (± SD) of 2 independent experiments. (B) Drug screen results show relative sensitivity and resistance of $p53^{KO}$ Nalm6 and RCH-ACV cells as visualized by area under curve (AUC) ratios. This ratio was calculated by dividing each $p53^{KO}$ cell line's AUC value of 3-(4,5-dimethylthiazol-2-yl)-2,5-diphenyltetrazolium bromide (MTT) conversion in response to 72 hours of treatment by that of its $p53^{WT}$ counterpart within cell lines; n = 1. GFP, green fluorescent protein.

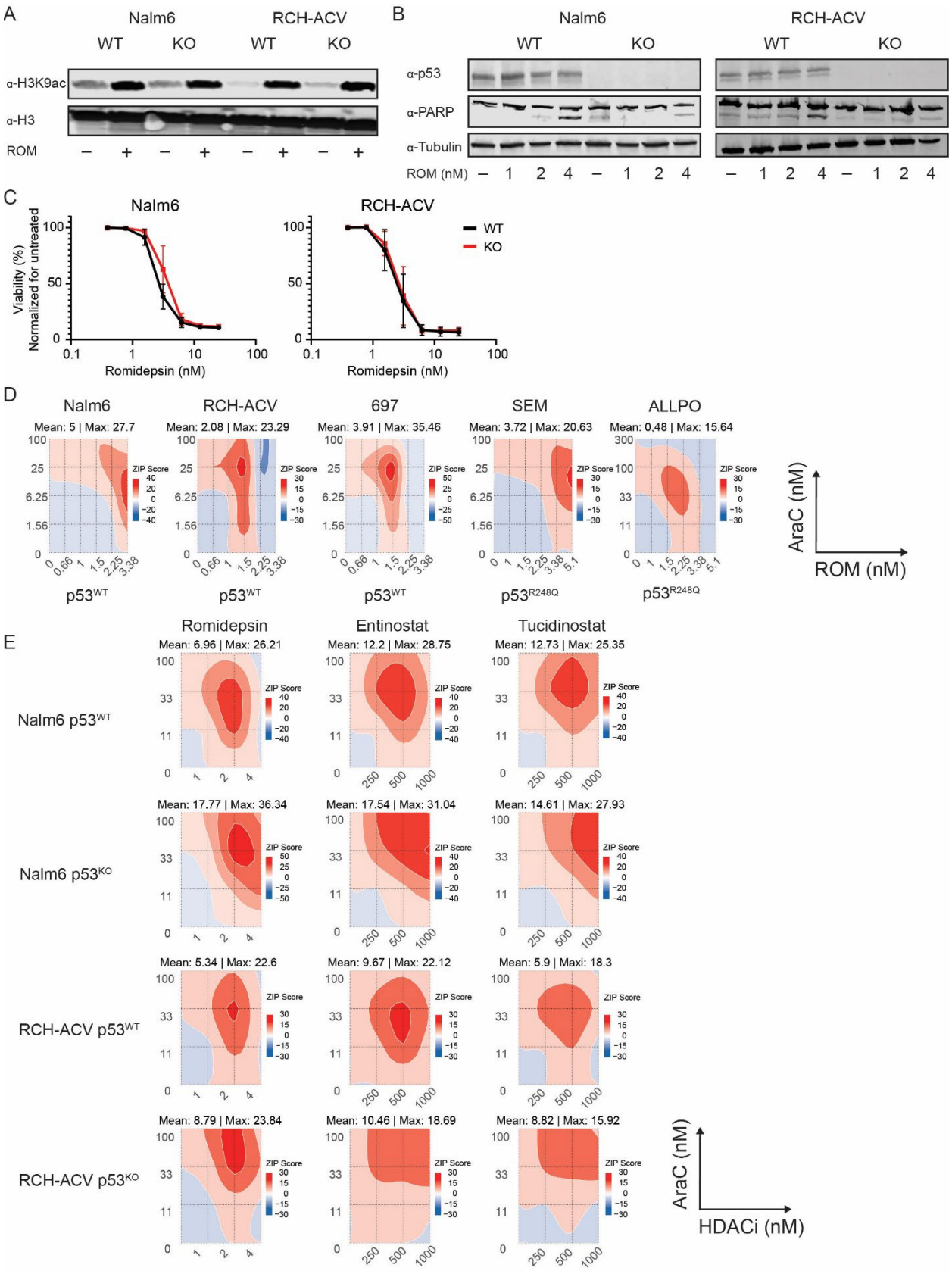
A
Nalm6
RCH-ACV
WT
KO
WT
KO
α-H3K9ac
α-H3
ROM
– + – + – + – +
B
Nalm6
RCH-ACV
WT
KO
WT
KO
α-p53
α-PARP
α-Tubulin
ROM (nM) – 1 2 4 – 1 2 4 – 1 2 4 – 1 2 4
C
Nalm6
RCH-ACV
WT
KO
Viability (%) Normalized for untreated
Romidepsin (nM)
Romidepsin (nM)
D
Nalm6
RCH-ACV
697
SEM
ALLPO
Mean: 5 | Max: 27.7
Mean: 2.08 | Max: 23.29
Mean: 3.91 | Max: 35.46
Mean: 3.72 | Max: 20.63
Mean: 0,48 | Max: 15.64
ZIP Score
p53WT
p53WT
p53WT
p53R248Q
p53R248Q
AraC (nM)
ROM (nM)
E
Romidepsin
Entinostat
Tucidinostat
Nalm6 p53WT
Mean: 6.96 | Max: 26.21
Mean: 12.2 | Max: 28.75
Mean: 12.73 | Max: 25.35
Nalm6 p53KO
Mean: 17.77 | Max: 36.34
Mean: 17.54 | Max: 31.04
Mean: 14.61 | Max: 27.93
RCH-ACV p53WT
Mean: 5.34 | Max: 22.6
Mean: 9.67 | Max: 22.12
Mean: 5.9 | Maxi: 18.3
RCH-ACV p53KO
Mean: 8.79 | Max: 23.84
Mean: 10.46 | Max: 18.69
Mean: 8.82 | Max: 15.92
ZIP Score
AraC (nM)
HDACi (nM)

Figure S2 - Romidepsin sensitizes p53-deficient and p53-proficient cells to cytarabine in vitro. (A) Western blot visualizing acetylated H3K9 expression in $p53^{WT}$ and $p53^{KO}$ cells in the presence or absence of 2 nM romidepsin for 48 hours, with total H3K9 as the loading control. A representative example of two independent experiments is shown. (B) Western blot visualizing p53 and PARP expression in romidepsin (2nM) treated $p53^{WT}$ and $p53^{KO}$ cells, with actin as the loading control. A representative example of three independent experiments is shown. (C) Dose-response curves showing cell viability of Nalm6 and RCH-ACV $p53^{WT}$ and $p53^{KO}$ cells treated with the indicated concentrations of romidepsin for 72 hours as determined by quantification of cells positive for amine-reactive dyes using flow cytometry. Each data point represents a mean (± SD) of 3 independent experiments. (D) *Zero interaction potency* (ZIP) synergy landscapes of the cell lines Nalm6, SEM, RCH-ACV, ALL-PO and 697, treated for 72 hours with the indicated concentrations of cytarabine and/or romidepsin. Quantification of cells positive for amine-reactive dyes using flow cytometry was used as a measure of viability and as input for synergy calculations, with data from three independent experiments. The p53 status of each cell line is included. (E) ZIP synergy landscapes of isogenic Nalm6 or RCH-ACV $p53^{WT}$ and $p53^{KO}$ models treated for 72 hours with the indicated concentrations of cytarabine and/or either romidepsin, entinostat, or tucidinostat. Quantification of cells positive for amine-reactive dyes using flow cytometry was used as a measure of viability and as input for synergy calculations, with data from three independent experiments. WT, wildtype; KO, knockout; H3K9ac, acetylated histone 3 lysine 9; H3, histone 3; PARP, poly-ADP ribose polymerase; AraC, cytarabine; ROM, romidepsin; HDACi, histone deacetylase inhibitor.

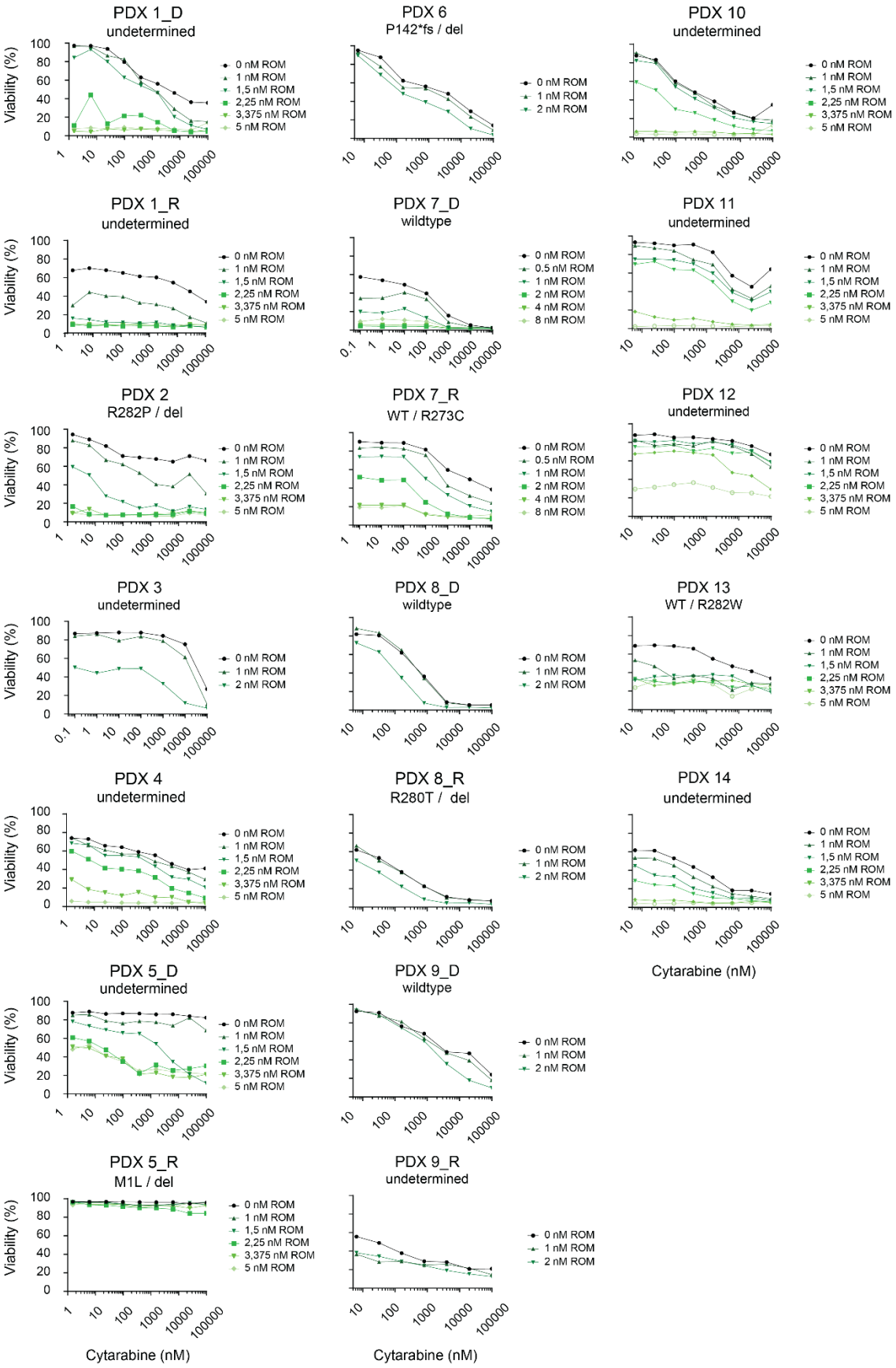
PDX 1_D
undetermined
PDX 6
P142*fs / del
PDX 10
undetermined
PDX 1_R
undetermined
PDX 7_D
wildtype
PDX 11
undetermined
PDX 2
R282P / del
PDX 7_R
WT / R273C
PDX 12
undetermined
PDX 3
undetermined
PDX 8_D
wildtype
PDX 13
WT / R282W
PDX 4
undetermined
PDX 8_R
R280T / _del
PDX 14
undetermined
PDX 5_D
undetermined
PDX 9_D
wildtype
PDX 5_R
M1L / del
PDX 9_R
undetermined
Viability (%)
Cytarabine (nM)
0 nM ROM
0.5 nM ROM
1 nM ROM
1,5 nM ROM
2 nM ROM
2,25 nM ROM
3,375 nM ROM
4 nM ROM
5 nM ROM
8 nM ROM

Figure S3 - Romidepsin sensitizes p53-deficient and p53-proficient patient-derived xenografts (PDX) to cytarabine *ex vivo*. Dose-response curves showing cell viability of nineteen ALL PDX samples seeded on hTERT-immortalized mesenchymal stromal cells and treated with the indicated concentrations of romidepsin and/or cytarabine for 72 hours. Diagnosis-relapse couples of the same patient are indicated by suffixes _D and _R, and TP53 status is included per PDX. Quantification of cells positive for amine-reactive dyes using flow cytometry was used as a measure of cell viability for one replicate. WT, wildtype; del, deleted; ROM, romidepsin.

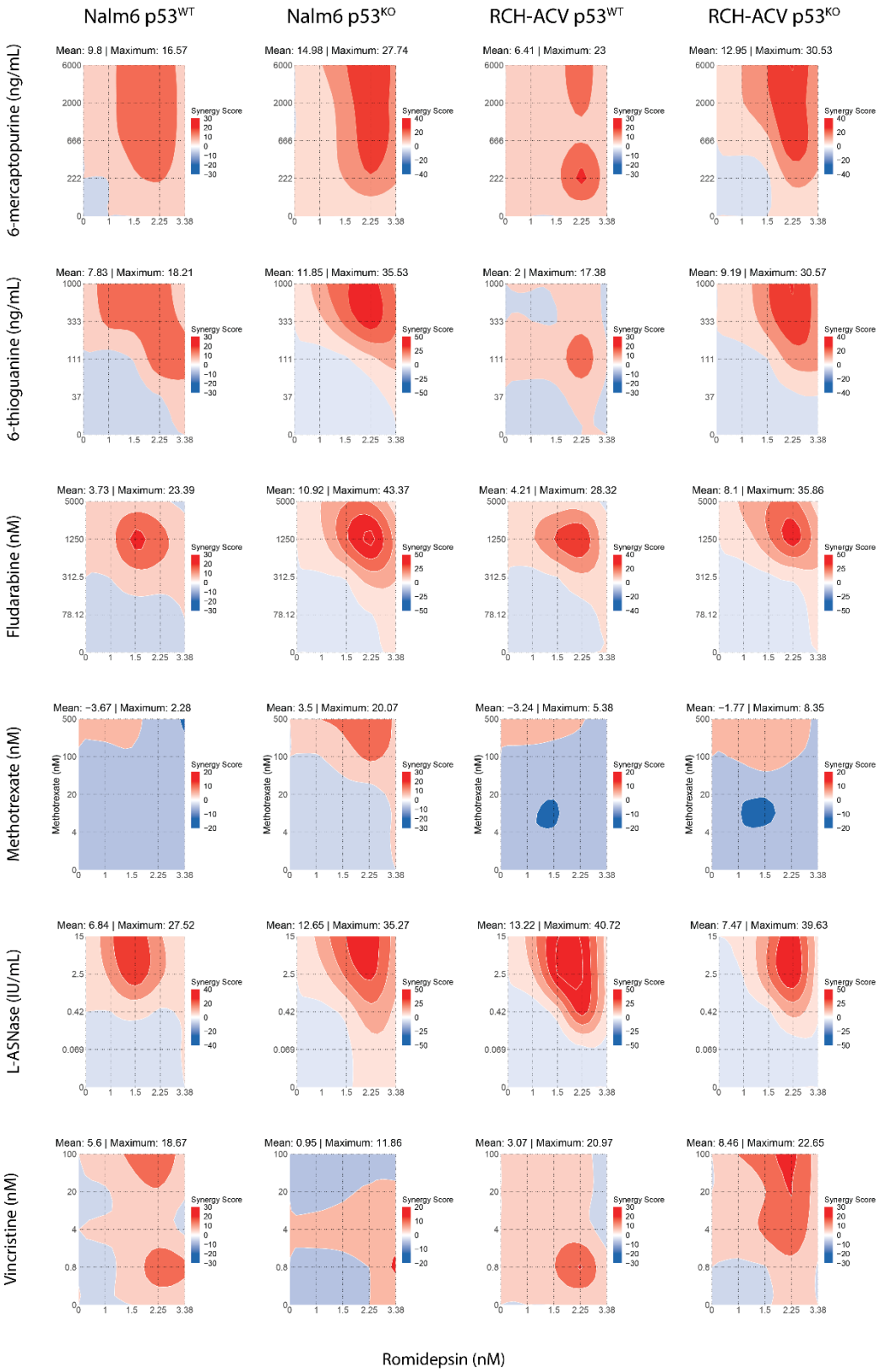
Nalm6 p53WT
Nalm6 p53KO
RCH-ACV p53WT
RCH-ACV p53KO
6-mercaptopurine (ng/mL)
Mean: 9.8 | Maximum: 16.57
Mean: 14.98 | Maximum: 27.74
Mean: 6.41 | Maximum: 23
Mean: 12.95 | Maximum: 30.53
6-thioguanine (ng/mL)
Mean: 7.83 | Maximum: 18.21
Mean: 11.85 | Maximum: 35.53
Mean: 2 | Maximum: 17.38
Mean: 9.19 | Maximum: 30.57
Fludarabine (nM)
Mean: 3.73 | Maximum: 23.39
Mean: 10.92 | Maximum: 43.37
Mean: 4.21 | Maximum: 28.32
Mean: 8.1 | Maximum: 35.86
Methotrexate (nM)
Mean: −3.67 | Maximum: 2.28
Mean: 3.5 | Maximum: 20.07
Mean: −3.24 | Maximum: 5.38
Mean: −1.77 | Maximum: 8.35
L-ASNase (IU/mL)
Mean: 6.84 | Maximum: 27.52
Mean: 12.65 | Maximum: 35.27
Mean: 13.22 | Maximum: 40.72
Mean: 7.47 | Maximum: 39.63
Vincristine (nM)
Mean: 5.6 | Maximum: 18.67
Mean: 0.95 | Maximum: 11.86
Mean: 3.07 | Maximum: 20.97
Mean: 8.46 | Maximum: 22.65
Synergy Score
Romidepsin (nM)

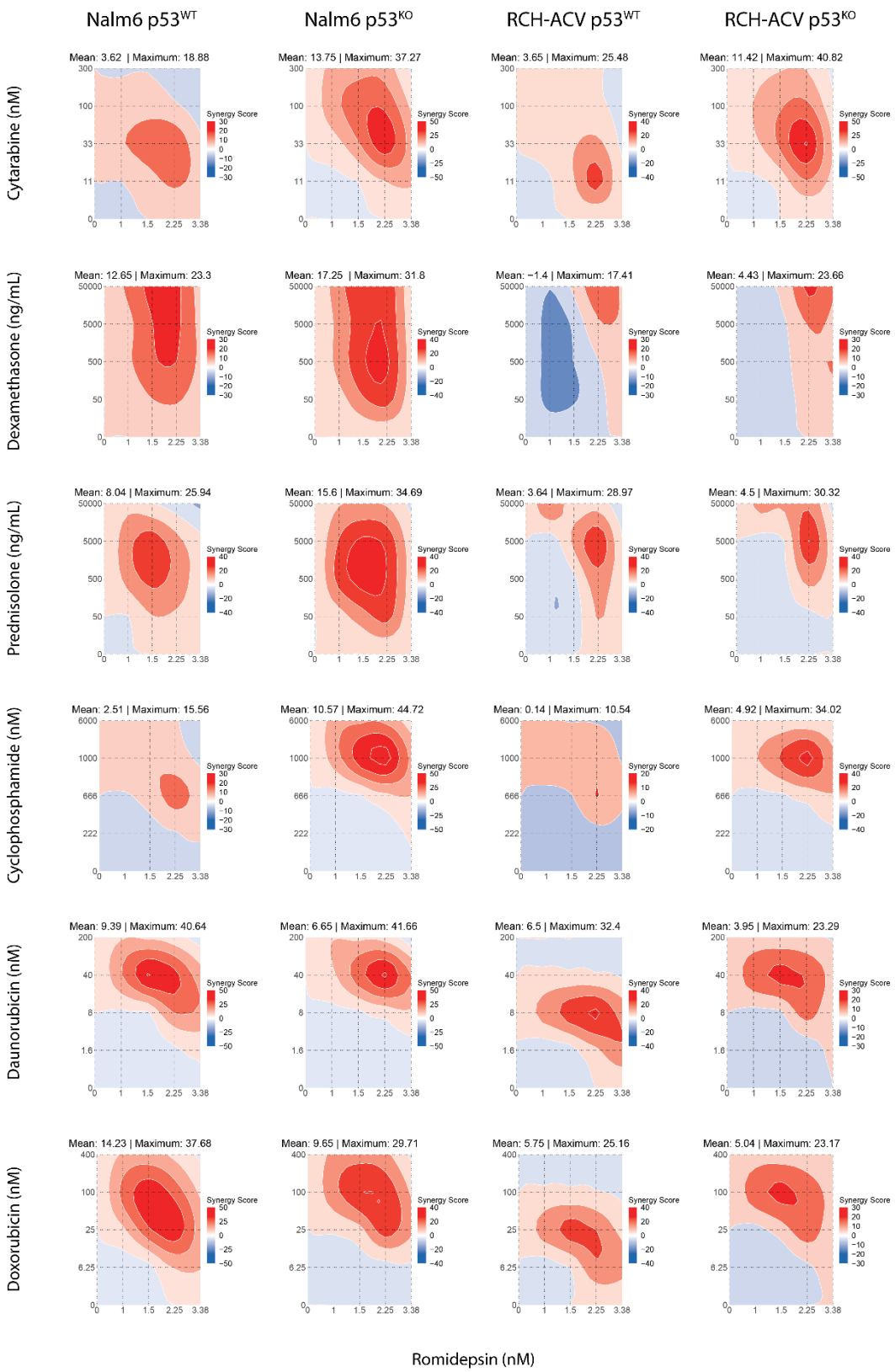
Nalm6 p53WT
Nalm6 p53KO
RCH-ACV p53WT
RCH-ACV p53KO
Cytarabine (nM)
Dexamethasone (ng/mL)
Prednisolone (ng/mL)
Cyclophosphamide (nM)
Daunorubicin (nM)
Doxorubicin (nM)
Romidepsin (nM)
Synergy Score
Mean: 3.62 | Maximum: 18.88
Mean: 13.75 | Maximum: 37.27
Mean: 3.65 | Maximum: 25.48
Mean: 11.42 | Maximum: 40.82
Mean: 12.65 | Maximum: 23.3
Mean: 17.25 | Maximum: 31.8
Mean: −1.4 | Maximum: 17.41
Mean: 4.43 | Maximum: 23.66
Mean: 8.04 | Maximum: 25.94
Mean: 15.6 | Maximum: 34.69
Mean: 3.64 | Maximum: 28.97
Mean: 4.5 | Maximum: 30.32
Mean: 2.51 | Maximum: 15.56
Mean: 10.57 | Maximum: 44.72
Mean: 0.14 | Maximum: 10.54
Mean: 4.92 | Maximum: 34.02
Mean: 9.39 | Maximum: 40.64
Mean: 6.65 | Maximum: 41.66
Mean: 6.5 | Maximum: 32.4
Mean: 3.95 | Maximum: 23.29
Mean: 14.23 | Maximum: 37.68
Mean: 9.65 | Maximum: 29.71
Mean: 5.75 | Maximum: 25.16
Mean: 5.04 | Maximum: 23.17

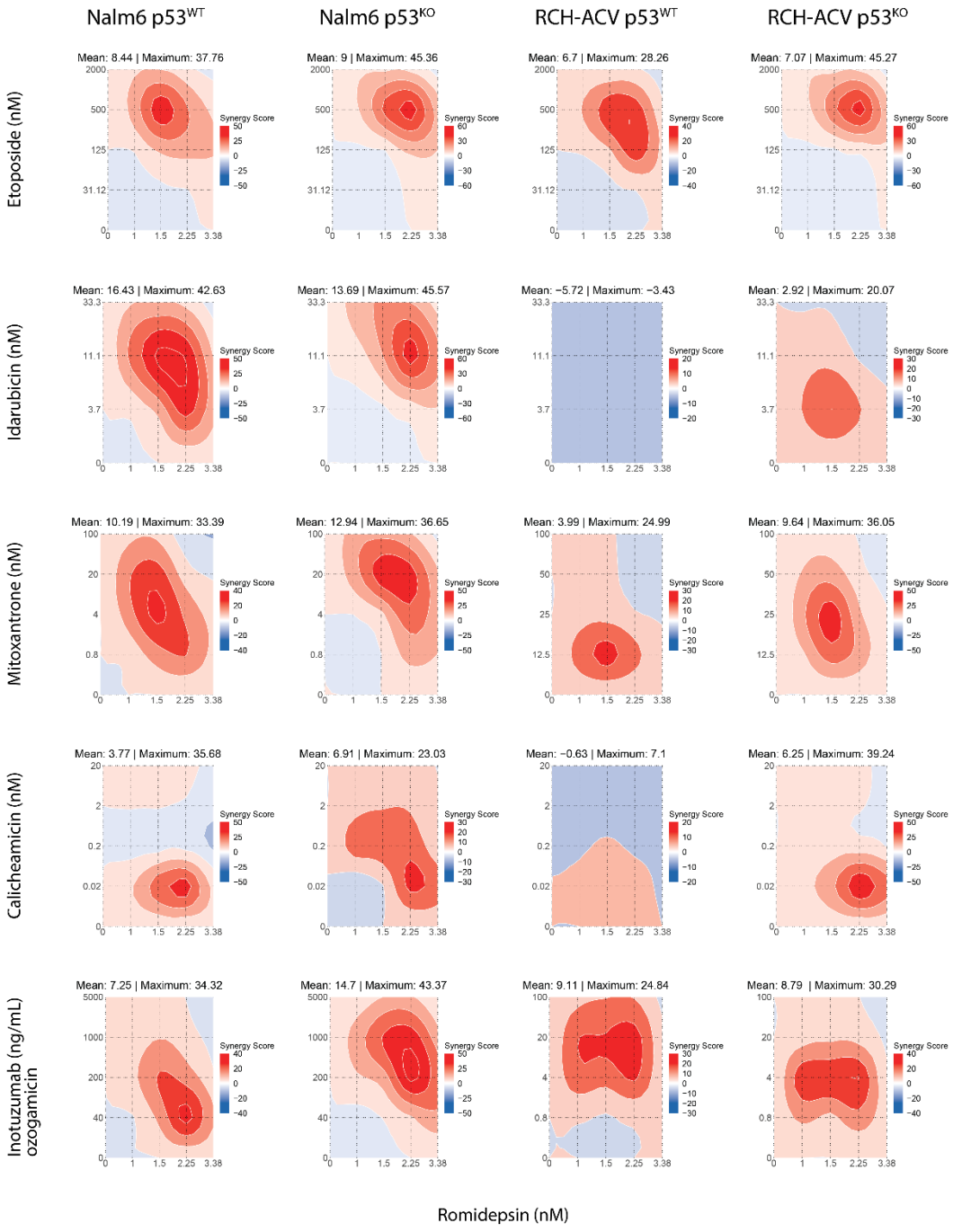

Figure S4 – Romidepsin synergizes with cytarabine in killing BCP-ALL cells. *Zero interaction potency* (ZIP) synergy landscapes of isogenic Nalm6 or RCH-ACV p53^{WT} and p53^{KO} models treated for 72 hours with the indicated concentrations of romidepsin and each one of 17 drugs currently used in BCP-ALL therapy. Quantification of cells positive for amine-reactive dyes using flow cytometry was used as a measure of viability and as input for synergy calculations, with data from two independent experiments. WT, wildtype; KO, knockout.

A

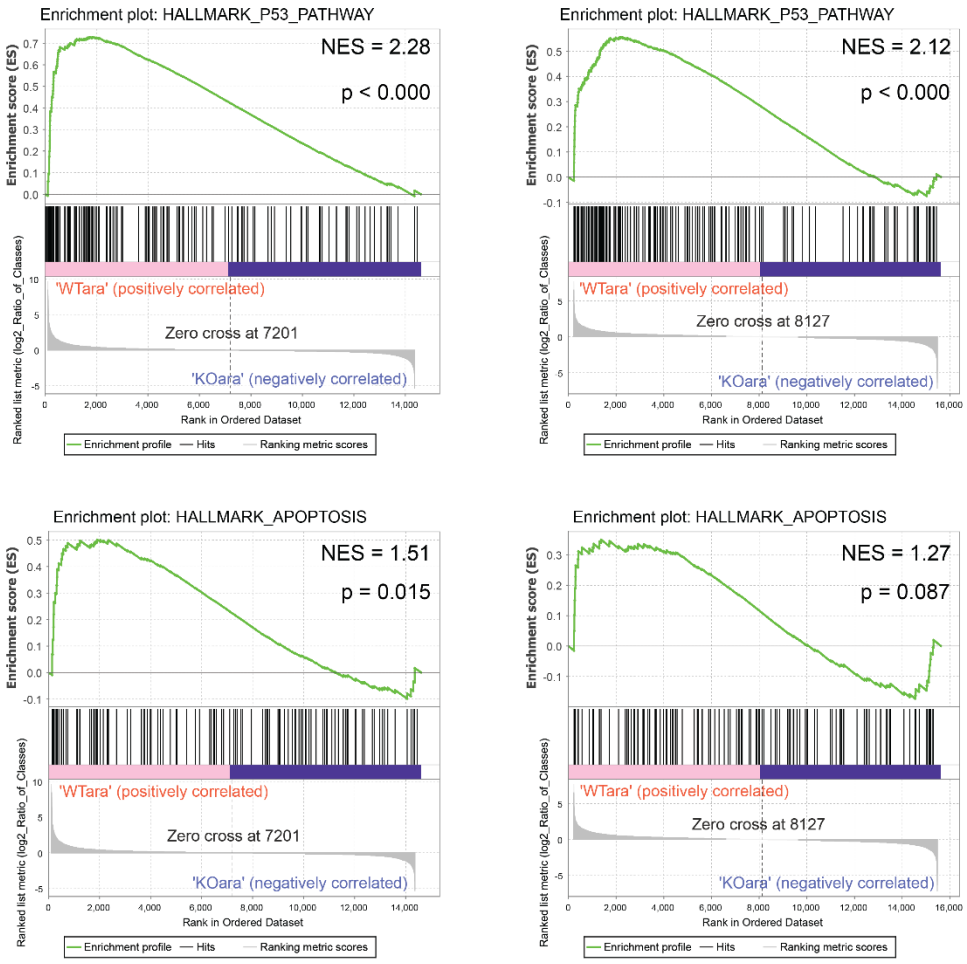
Nalm6
RCH-ACV
Enrichment plot: HALLMARK_P53_PATHWAY
NES = 2.28
p < 0.000
'WTara' (positively correlated)
Zero cross at 7201
'KOara' (negatively correlated)
Enrichment plot: HALLMARK_P53_PATHWAY
NES = 2.12
p < 0.000
'WTara' (positively correlated)
Zero cross at 8127
'KOara' (negatively correlated)
Enrichment plot: HALLMARK_APOPTOSIS
NES = 1.51
p = 0.015
'WTara' (positively correlated)
Zero cross at 7201
'KOara' (negatively correlated)
Enrichment plot: HALLMARK_APOPTOSIS
NES = 1.27
p = 0.087
'WTara' (positively correlated)
Zero cross at 8127
'KOara' (negatively correlated)
Enrichment score (ES)
Ranked list metric (log2_Ratio_of_Classes)
Rank in Ordered Dataset
Enrichment profile
Hits
Ranking metric scores

B

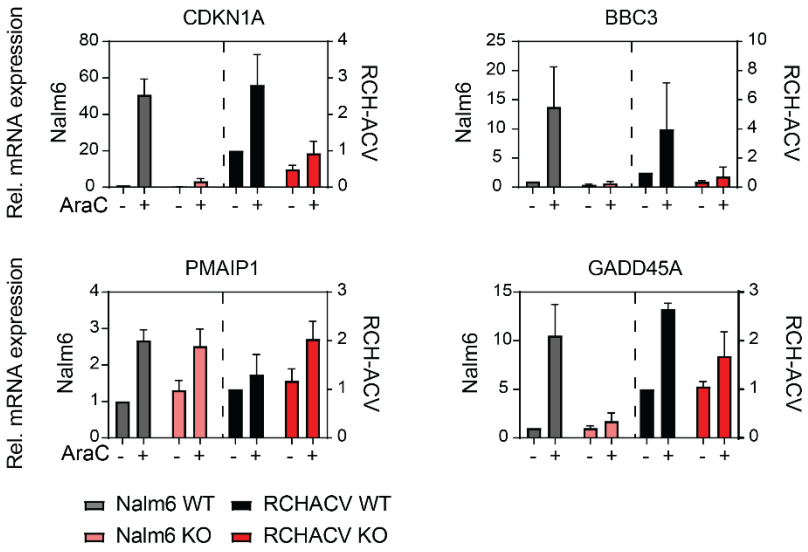
CDKN1A
BBC3
PMAIP1
GADD45A
Rel. mRNA expression
Nalm6
RCH-ACV
AraC
Nalm6 WT
RCHACV WT
Nalm6 KO
RCHACV KO

Figure S5 – p53 loss abrogates induction of p53-mediated transcriptional effects upon cytarabine treatment. (A) Gene Set Enrichment Analysis plots were generated for the comparison of cytarabine-treated $p53^{WT}$ versus $p53^{KO}$ cells in Nalm6 and RCH-ACV. Plots are shown for HALLMARK_P53_PATHWAY and HALLMARK_APOPTOSIS gene sets. (B) mRNA levels of CDKN1A, BBC3, PMAIP1 and GADD45a were assessed by real-time qPCR after treatment with 200 nM cytarabine for 16 hours. Data are mean ± SD from two technical replicates each for three biological replicates. NES, Normalized Enrichment Score; CDKN1A, cyclin dependent kinase 1A; BBC3, BCL2 binding component 3; PMAIP1, phorbol-12-myristate-13-acetate-induced protein 1; GADD45A, growth arrest and DNA damage inducible alpha; qPCR, quantitative real-time polymerase chain reaction; AraC/ara, cytarabine; WT, wildtype; KO, knockout.

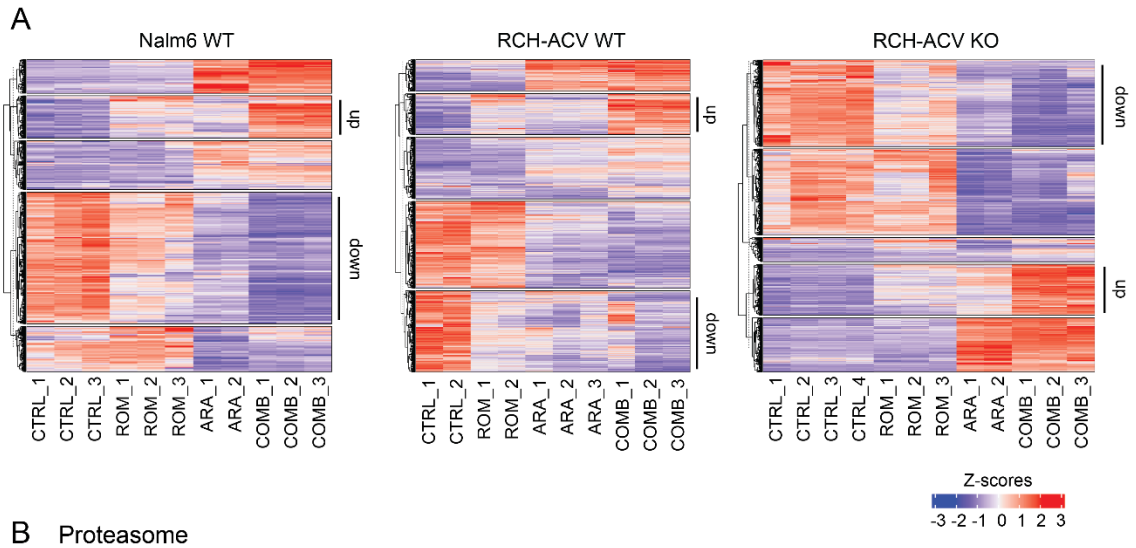
A
Nalm6 WT
RCH-ACV WT
RCH-ACV KO
up
down
CTRL_1
CTRL_2
CTRL_3
ROM_1
ROM_2
ROM_3
ARA_1
ARA_2
COMB_1
COMB_2
COMB_3
Z-scores
-3 -2 -1 0 1 2 3

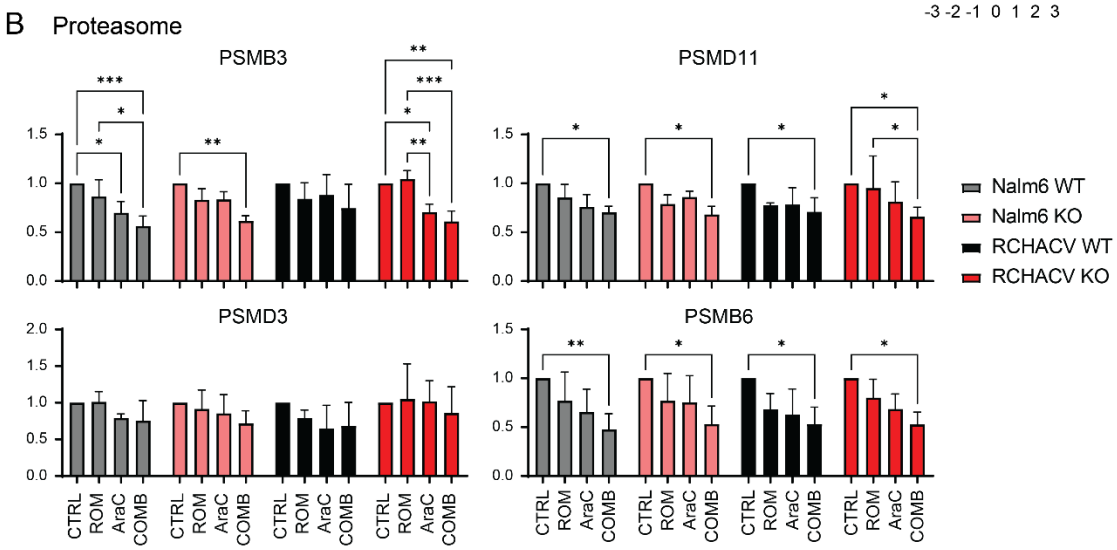
B Proteasome
PSMB3
PSMD11
PSMD3
PSMB6
CTRL
ROM
AraC
COMB
Nalm6 WT
Nalm6 KO
RCHACV WT
RCHACV KO

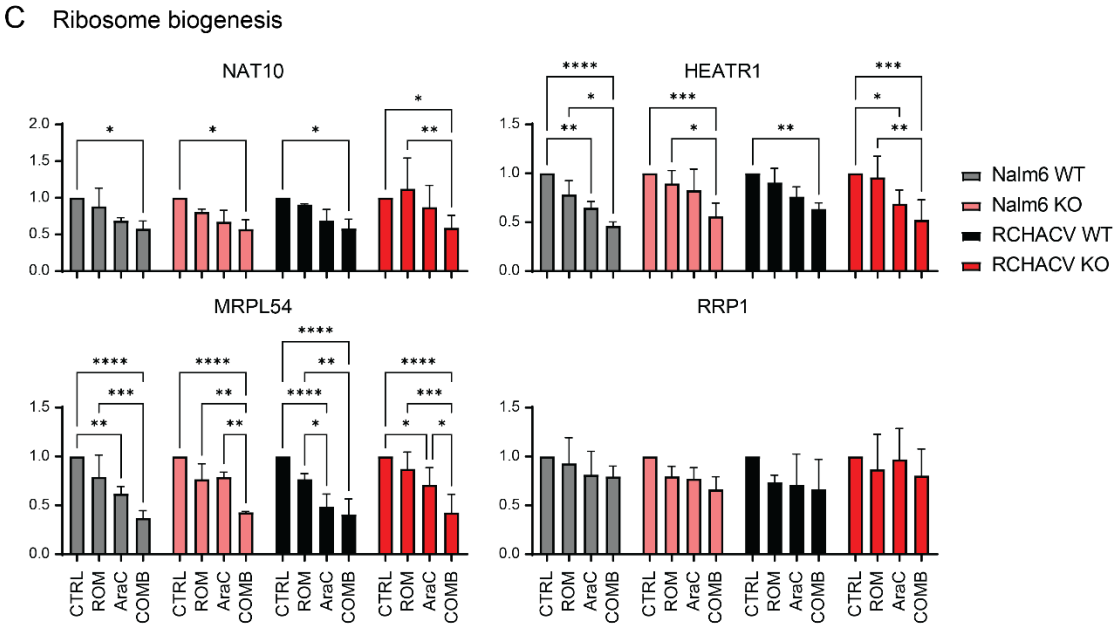
C Ribosome biogenesis
NAT10
HEATR1
MRPL54
RRP1
CTRL
ROM
AraC
COMB
Nalm6 WT
Nalm6 KO
RCHACV WT
RCHACV KO

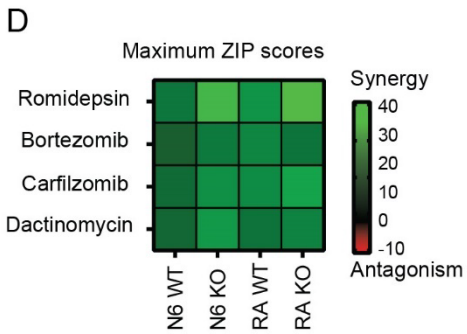

Figure S6 – Romidepsin and cytarabine modulate RNA expression in p53 proficient and deficient cell lines. (A) Heat maps showing gene-expression levels from RNA-seq analysis in $p53^{WT}$ (Nalm6 and RCH-ACV) and $p53^{KO}$ (RCH-ACV) cells treated with cytarabine and/or romidepsin. Differentially expressed gene calculation was performed for every treatment combination within cell lines and filtered for genes with a p-value of less than 0.05 and a log2 cut-off of smaller than -0.5 or greater than 0.5. Gene lists were then combined for both genotypes per cell line, z-scores were computed and heatmaps were generated for each model in RStudio using unsupervised clustering. Clusters of up- (up) and downregulated (down) genes in both romidepsin vs control treatment and combination vs cytarabine treatment comparisons are indicated. (B-C) mRNA levels of PSMB3, PSMD11, PSMD3, PSMB6 (B), NAT10, HEATR1, MRPL54 and RRP1 (C) assessed by real-time qPCR after treatment with 2 nM romidepsin and/or 200 nM cytarabine for 16 hours. Data are mean ± SD from two technical replicates each for three biological replicates. Differences in expression between the treatment conditions were tested for significance per model using a two-way ANOVA per followed by Tukey's multiple comparisons test. (D) Heatmap of maximum *zero interaction potency* (ZIP) synergy scores for 2 independent experiments. Nalm6 and RCH-ACV $p53^{KO}$ cells were exposed to five concentrations of romidepsin and five concentrations of the drug listed per row for 72 hours. Quantification of cells positive for amine-reactive dyes using flow cytometry was used as a measure of viability and as input for synergy calculations. CTRL, control treatment; ROM, romidepsin; AraC/ARA, cytarabine; COMB, combination treatment; N6, Nalm6; RA, RCH-ACV; WT, wildtype; KO, knockout. *$p < 0.05$; **$p < 0.01$; ***$P < 0.001$, ****$p < 0.0001$.

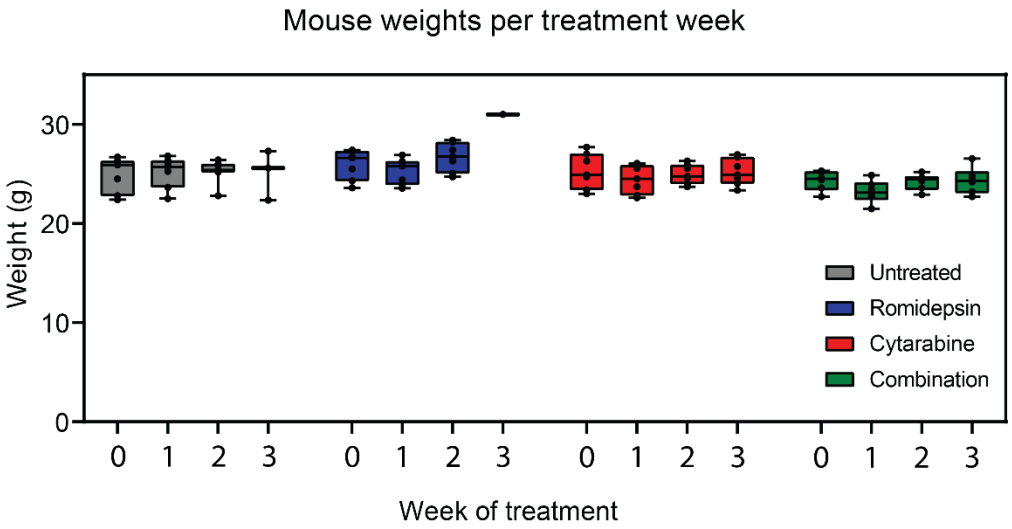

Figure S7 - Mouse weights for in vivo experiment. Luciferase-expressing RCH-ACV p53^{KO} cells were injected into NRG-SM3 mice that were treated for three weeks with either cytarabine, romidepsin or the combination. Mouse weights are visualized per treatment week.

Table S1 - Information on primers, plasmids and antibodies used in this manuscript. TP53, tumor protein 53; CDKN1A, cyclin dependent kinase 1A; BBC3, BCL2 binding component 3; PUMA, p53 upregulated modulator of apoptosis; PMAIP1, phorbol-12-myristate-13-acetate-induced protein 1; GADD45A, growth arrest and DNA damage inducible alpha; PSMB, proteasome subunit beta; PSMD, proteasome subunit delta; NAT, N-acetyltransferase 10; HEATR1, HEAT repeat containing 1; MRPL54, mitochondrial ribosomal protein L54; RRP1, ribosomal RNA processing 1; GFP, green fluorescent protein; PARP, poly-ADP ribose polymerase; gRNA, guide RNA; qPCR, quantitative real-time polymerase chain reaction; TBS, TRIS-buffered saline.

Oligo		
Target gene (protein)	**Application**	**Target sequence**
***TP53* (p53)**	gRNA targeting ex. 5	CAACAAGATGTTTTGCCAAC
	gRNA targeting ex. 5	CAGGGCAGGTCTTGGCCAGT
	qPCR fw	TGGAGTATTTGGATGACAGAAACA
	qPCR rev	TGTAGTGGATCGTGGTACAGTCAG
***CDKN1A* (p21)**	qPCR fw	CAGGTGGACCTGGAGACTCTCAGG
	qPCR rev	AGACTAAGGCAGAAGATGTAGAGC
***BBC3* (PUMA)**	qPCR fw	GACCTCAACGCACAGTACGAG
	qPCR rev	AGGAGTCCCATGATGAGATTGT
***PMAIP1* (NOXA)**	qPCR fw	CTGGAAGTCGAGTGTGCTACTC
	qPCR rev	TGAAGGAGTCCCCTCATGCAAG
***GADD45A* (GADD45a)**	qPCR fw	CCTGTGAGTGAGTGCAGAAA
	qPCR rev	AGCCGAGAATTCCTCCAAAG
***PSMB3* (PSMB3)**	qPCR fw	TTCCGGCTGAACCTGTATGAG
	qPCR rev	GTAAGGGCCAAACCGTTTCTC
***PSMD11* (PSMD11)**	qPCR fw	GCCTCCATCGACATCCTCC
	qPCR rev	GAGCTGCTTTAGCCTTGCTG
***PSMD3* (PSMD3)**	qPCR fw	CGCCTCAACCACTATGTTCTG
	qPCR rev	GGACGGAACTGTAAATCAGCC
***PSMB6* (PSMB6)**	qPCR fw	GGCTACCTTACTAGCTGCTCG
	qPCR rev	GATTGGCGATGTAGGACCCAG
***NAT10* (NAT10)**	qPCR fw	ATAGCAGCCACAAACATTCGC
	qPCR rev	ACACACATGCCGAAGGTATTG
***HEATR1* (HEATR1)**	qPCR fw	GCCCTCCCTCAAAGTGATGC
	qPCR rev	CGCTTCCTTAGGGTCAAATAACA
***MRPL54* (MRPL54)**	qPCR fw	GCGACCAAACGCCTTTTCG
	qPCR rev	GATCTGTGCATACGTCGGGG
***RRP1* (RRP1)**	qPCR fw	CAGGTGGTTTTACGCACGAC

	qPCR rev		GAACGAGCTGGGAAATAGTCC		
Plasmids					
Application	**Supplier**	**Insert**	**Plasmid**		
GFP and luciferase-expressing cells	Gifted by Prof. Saha, University of Manchester	GFP-luciferase	pLNT-SFFV		
mCherry- and luciferase-expressing cells	Gifted by Prof. Saha, University of Manchester	mCherry-luciferase	pLNT-SFFV		
Genomic knockout	Addgene, #PX458	gRNA	pSpCas9-2A-GFP		
Primary antibodies					
Target	**Host**	**Supplier**	**Cat. number**	**Solvent**	**Dilution**
p53	Mouse	Santa Cruz Biotechnology	sc-126	1% milk in TBS	1:1.000
p21	Rabbit	Cell Signaling Technologies	2947	1% milk in TBS	1:1.000
PARP	Rabbit	Cell Signaling Technologies	9542	1% milk in TBS	1:4.000
PUMA	Rabbit	Cell Signaling Technologies	12450	1% milk in TBS	1:1.000
Tubulin	Rabbit	Cell Signaling Technologies	2148	1% milk in TBS	1:5.000
Actin	Mouse	Santa Cruz Biotechnology	sc-69879	1% milk in TBS	1:5.000-1:10.000
Vinculin	Mouse	Sigma Aldrich	V9131	1% milk in TBS	1:4.000
Secondary antibodies					
Anti-mouse IgG Ab 680RD	Goat	LI-COR	926-68070	1% milk in TBS	1:5000
Anti-mouse IgG Ab 800CW	Goat	LI-COR	926-32210	1% milk in TBS	1:5000
Anti-rabbit IgG Ab 680RD	Goat	LI-COR	926-68071	1% milk in TBS	1:5000
Anti-rabbit IgG Ab 800CW	Goat	LI-COR	926-32211	1% milk in TBS	1:5000

Table S2 – Single-cell clone and patient-derived xenograft genotypes. For cell line models, nucleotide, amino acid, and genotype results of the TP53 gene of Nalm6 and RCH-ACV wildtype and knockout clones after CRISPR/Cas9 targeting of exon 5 as determined by Sanger sequencing. For patient-derived xenografts, copy number and mutation status are shown. PDX, patient-derived xenograft; WT, wildtype; KO, knockout; undet, undetermined; D, diagnosis; R, relapse.

Cell line models					
Model	**Clone**	**Allele**	**Nucleotide**	**Amino acid**	**Genotype**
Nalm6	1	Both	Unchanged	Unchanged	WT
	2	Both	Unchanged	Unchanged	
	5	Both	Unchanged	Unchanged	
	8	Both	Unchanged	Unchanged	
	11	Both	Unchanged	Unchanged	
	30	1	c.406_407insG	p.Gln136fs	KO
		2	c.406_407insGGT	p.Gln136fs	
	31	1	c.406_407insGGT	p.Gln136fs	
		2	c.406_407insG	p.Gln136fs	
	37	1	c.406_407insGGT	p.Gln136fs	
		2	c.406_407insG	p.Gln136fs	
RCH-ACV	67	Both	Unchanged	Unchanged	WT
	69	Both	Unchanged	Unchanged	
	96	Both	Unchanged	Unchanged	
	110	Both	Unchanged	Unchanged	
	90	1	c.411_412insTGAA	p.Ala138fs	KO
		2	c.411_412insTGAA	p.Ala138fs	
	107	1	c.412_413insG	p.Ala138fs	
		2	c.412_413insG	p.Ala138fs	
	108	1	c.412_413insG	p.Ala138fs	
		2	c.410_411insAGGC	p.Leu137fs	

Patient-derived xenografts				
Sample	**Status**	**Copy number**	**Mutation status**	**Pathogenicity of mutation**
PDX 1_D	Undet	Undet	Undet	
PDX 1_R	Undet	Undet	Undet	
PDX 2	Aberrant	Monoallelic loss	p.R282P	Yes, hotspot[10]
PDX 3	Undet	Undet	Undet	

PDX 4	Undet	Undet	Undet	
PDX 5_D	Undet	Undet	Undet	
PDX 5_R	Aberrant	Monoallelic loss	p.M1L	Yes, loss of start codon
PDX 6	Aberrant	Monoallelic loss	p.P142*fs	Yes, frameshift
PDX 7_D	Wildtype	WT	WT	
PDX 7_R	Aberrant	WT	R273C	Yes, hotspot [10]
PDX 8_D	Wildtype	WT	WT	
PDX 8_R	Aberrant	Monoallelic loss	p.R280T	Yes [11, 12]
PDX 9_D	Wildtype	WT	WT	
PDX 9_R	Undet	Undet	Undet	
PDX 10	Undet	Undet	Undet	
PDX 11	Undet	Undet	Undet	
PDX 12	Undet	Undet	Undet	
PDX 13	Aberrant	WT	R282W	Yes, hotspot [10]
PDX 14	Undet	Undet	Undet	

Table S3 – Extended gene set enrichment results. For each result, the used gene set, comparison, cell line, normalized enrichment score, p-value and false discovery rate q-value are shown. WT, wildtype; KO, knockout; NES, normalized enrichment score; FDR, false discovery rate.

Gene set: HALLMARK_APOPTOSIS			
Comparison: Romidepsin versus control treatment			
Cell line	**Normalized Enrichment Score (NES)**	**p-value**	**FDR q-value**
Nalm6 WT	1.55	0.002	0.015
Nalm6 KO	1.46	0.014	0.040
RCHACV WT	1.23	0.133	0.248
RCHACV KO	1.48	0.002	0.024
Gene set: HALLMARK_APOPTOSIS			
Comparison: Combination versus cytarabine			
Cell line	**Normalized Enrichment Score (NES)**	**p-value**	**FDR q-value**
Nalm6 WT	1.31	0.06	0.147
Nalm6 KO	1.49	0.008	0.033
RCHACV WT	1.33	0.018	0.081
RCHACV KO	1.46	0.001	0.026
Gene set: HALLMARK_P53_PATHWAY			
Comparison: Romidepsin versus control treatment			
Cell line	**Normalized Enrichment Score (NES)**	**p-value**	**FDR q-value**
Nalm6 WT	1.2	0.13	0.28
Nalm6 KO	1.26	0.079	0.19
RCHACV WT	1.01	0.465	0.585
RCHACV KO	1.21	0.108	0.201
Gene set: HALLMARK_P53_PATHWAY			
Comparison: Combination versus cytarabine			
Cell line	**Normalized Enrichment Score (NES)**	**p-value**	**FDR q-value**
Nalm6 WT	-0.75	1	1
Nalm6 KO	1.37	0.021	0.072
RCHACV WT	1.03	0.419	0.623
RCHACV KO	1.46	0.001	0.026

REFERENCES

1. Schmitz M, Breithaupt P, Scheidegger N, et al. Xenografts of highly resistant leukemia recapitulate the clonal composition of the leukemogenic compartment. Blood. 2011;118(7):1854-1864.

2. Zheng S, Wang W, Aldahdooh J, et al. SynergyFinder Plus: Toward Better Interpretation and Annotation of Drug Combination Screening Datasets. Genomics Proteomics Bioinformatics. 2022;20(3):587-596.

3. Ritz C, Baty F, Streibig JC, Gerhard D. Dose-Response Analysis Using R. PLoS One. 2016;10(12):e0146021.

4. Subramanian A, Tamayo P, Mootha VK, et al. Gene set enrichment analysis: A knowledge-based approach for interpreting genome-wide expression profiles. Proc Natl Acad Sci U S A. 2005;102(43):15545-15550.

5. Mootha VK, Lindgren CM, Eriksson K-F, et al. PGC-1α-responsive genes involved in oxidative phosphorylation are coordinately downregulated in human diabetes. Nat Genet. 2003;34(3):267-273.

6. Bioinformatics UGent. Calculate and draw custom Venn diagrams. https://bioinformatics.psb.ugent.be/webtools/Venn/. Accessed April 18, 2023.

7. Love MI, Huber W, Anders S. Moderated estimation of fold change and dispersion for RNA-seq data with DESeq2. Genome Biol. 2014;15(12).

8. Szklarczyk D, Kirsch R, Koutrouli M, et al. The STRING database in 2023: protein-protein association networks and functional enrichment analyses for any sequenced genome of interest. Nucleic Acids Res. 2023;51(D1):D638-D646.

9. Gu Z. Complex heatmap visualization. Imeta. 2022;1(3):e43.

10. McLeod C, Gout AM, Zhou X, et al. St. Jude Cloud: A Pediatric Cancer Genomic Data-Sharing Ecosystem. Cancer Discov. 2021;11(5):1082-1099.

11. Lin C, Liang Y, Zhu H, Zhang J, Zhong X. R280T mutation of p53 gene promotes proliferation of human glioma cells through GSK-3β/PTEN pathway. Neurosci Lett. 2012;529(1):60-65.

12. Qin ZQ, Li QG, Yi H, et al. Heterozygous p53-R280T Mutation Enhances the Oncogenicity of NPC Cells Through Activating PI3K-Akt Signaling Pathway. Front Oncol. 2020;10.